



Total Ionizing Dose Test Report

No. 12T-RTAX2000S-CG624-D63WS1

September 24, 2012

Table of Contents

I.	Summary Table.....	3
II.	Total Ionizing Dose (TID) Testing.....	3
A.	Device-Under-Test (DUT) and Irradiation Parameters	3
B.	Test Method	4
C.	Design and Parametric Measurements.....	5
III.	Test Results	6
A.	Functionality	6
B.	Power Supply Current (ICCA and ICCI).....	6
C.	Single-Ended Input Logic Threshold (VIL/VIH).....	10
D.	Differential Input (LVPECL) Threshold Voltage (VIL/VIH)	12
E.	Output-Drive Voltage (VOL/VOH)	13
F.	Propagation Delay.....	16
G.	Transition Characteristics.....	18
	Appendix A: DUT Design Schematics.....	30

TOTAL IONIZING DOSE TEST REPORT

No. 12T-RTAX2000S-CG624-D63WS1

September 24, 2012

CK Huang and J.J. Wang

(408) 643-6136, (408) 643-6302

chang-kai.huang@microsemi.com, jih-jong.wang@microsemi.com

I. Summary Table

Parameter	Tolerance
1. Gross Functionality	Passed 300 krad (SiO_2)
2. Power Supply Current (ICCA/ICCI)	Passed 200 krad (SiO_2)
3. Input Threshold (VIL/VIH)	Passed 300 krad (SiO_2)
4. Output Drive (VOL/VOH)	Passed 300 krad (SiO_2)
5. Propagation Delay	Passed 300 krad (SiO_2) for 10% degradation criterion
6. Transition Characteristics	Passed 300 krad (SiO_2)

II. Total Ionizing Dose (TID) Testing

This testing is designed on the base of an extensive database (see TID data of antifuse-based FPGAs at <http://www.klabs.org> and <http://www.microsemi.com/soc>) accumulated from the TID testing of many generations of antifuse-based FPGAs.

A. Device-Under-Test (DUT) and Irradiation Parameters

Table 1 lists the DUT and irradiation parameters. During irradiation and annealing, each input is grounded.

Table 1 DUT and Irradiation Parameters

Part Number	RTAX2000S
Package	CG624
Foundry	United Microelectronics Corp.
Technology	0.15 μm CMOS
DUT Design	Rtax2000_CG624_Top
Die Lot Number	D63WS1
Quantity Tested	6
Serial Number	300 krad(SiO_2): 5318, 5319, 5320 200 krad(SiO_2): 5321, 5355, 5356
Radiation Facility	Defense Microelectronics Activity
Radiation Source	Co-60
Dose Rate ($\pm 5\%$)	7.5 krad(SiO_2)/min
Irradiation Temperature	Room
Irradiation and Measurement Bias (VCCI/VCCA)	Static at 3.3 V/1.5 V

B. Test Method

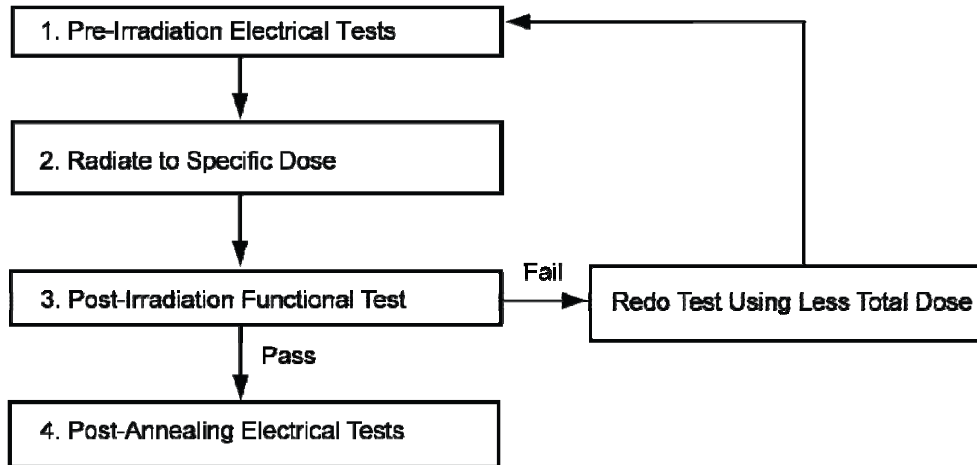


Figure 1 Parametric Test Flow Chart

The test method generally follows the guidelines in the military standard TM1019.8. Figure 1 is the flow chart describing the steps for functional and parametric tests, irradiation, and post-irradiation annealing.

The accelerated aging, or rebound test mentioned in TM1019.8 is unnecessary because there is no adverse time-dependent effect (TDE) in Microsemi products manufactured by deep sub-micron CMOS technologies. Elevated temperature annealing basically reduces the effects originating from radiation-induced leakage currents. As indicated by test data in the following sections, the predominant radiation effects in RTAX2000S are due to radiation-induced leakage currents.

Room temperature annealing is performed in this test; the duration is approximately 3 weeks.

C. Design and Parametric Measurements

The DUT uses a high utilization generic design, rtax2000_CG624_Top, for testing total dose effects. These logic designs are described in the following subsections. Appendix A shows the block diagram.

Generally, the functional test is performed on every design; most inputs are tested for threshold voltage and leakage current, including global clocks; the standby I_{CC} includes I_{CCI} and I_{CCA} . Except propagation delay and the transition characteristic, which is measured on the output O_BS, all other parameter measurements are done on a tester. Also note that, due to logistics limitation, the post-irradiation but pre-room-temperature-annealing functional test is performed on bench; the tested designs are shift registers and long buffer string, which are design 5 and 6 described in the following.

1. Embedded SRAM

This design is to test the function of the embedded SRAM. It uses all the RAM blocks available in the DUT. This design enables an automatic testing sequence that every bit is written and then read. Any error will be reported as a signal in the output.

2. Unidirectional LVTTL Input and Output

This is for testing radiation effects on unidirectional input and output threshold, leakage, and buffer fan-out. There are 3 sub-designs: a) a logic-core buffer with 8 fan-outs; b) a logic-core buffer with 3 fan-outs; c) 6 channels of input buffer directly connected to output buffer without core logic. LVTTL is used because it is the worst case among all the single-ended standards.

3. Bidirectional LVTTL IO

This design is for testing the radiation effects on the input/output characteristic of the bidirectional IO. There are 7 channels of bidirectional IO for radiation effects testing.

4. LVPECL Input

This design is for testing the radiation effects on the LVPECL differential inputs. 3.3V-LVPECL is considered the worst case differential input standard in the DUT. There are 7 channels.

5. Shift Registers

This design is to test the radiation effects on the function of flip-flops, which are configured R-Cells. There are 4 shift registers and each using a different global clock; one has 3,584 bits and the other three each has 2,048 bits.

6. Long Buffer String

This design is to measure the radiation effects on the propagation delay. The input of the design using a clock feeding a toggle flip-flop to generate a checkerboard signal; this signal is then fed into a buffer string with 10,000 stages. The time delay between the input clock edge at CLOCK_IN and the output switching due to this clock edge at O_BS is defined as propagation delay high to low (T_{pdhl}) or low to high (T_{pdlh}); the percentage change of the average of T_{pdhl} and T_{pdlh} is used to determine the radiation effects. A more than 10% of propagation change is considered as failure.

III. Test Results

A. Functionality

Every DUT passed the pre-irradiation and post-annealing functional tests. The as-irradiated DUT is functionally tested on the output (O_FF_HCLKA) of the largest shift register.

B. Power Supply Current (ICCA and ICCI)

Figure 2 through Figure 7 plot the influx standby ICCA and ICCI versus total dose for each DUT. The post-annealing ICC for four different bit patterns, all '0', all '1', checkerboard and inverted-checkerboard, in the RAM are basically the same.

In compliance with TM1019.8 subsection 3.11.2.c, the post-irradiation-parametric limit (PIPL) for the post-annealing ICCI in this test is defined as the addition of highest ICCI, ICCDA and ICCDIFFA values in Table 2-4 of the *RTAX-S/SL and RTAX-DSP Radiation-Tolerant FPGAs* datasheet:

http://www.microsemi.com/soc/documents/RTAXS_DS.pdf

For ICCA, the PIPL is 500 mA; the PIPL of ICCI equals to $35 + 10 + 3.13 \times 7 = 66.91$ (mA). Note that there are 7 pairs of differential LVPECL inputs in each DUT.

Table 2 summarizes the pre-irradiation, post-irradiation right after irradiation and before anneal, and post-annealing ICCA and ICCI data.

Table 2 Pre-irradiation, Post Irradiation and Post-Annealing ICC

DUT	Total Dose	ICCA (mA)			ICCI (mA)		
		Pre-irrad	Post-irrad	Post-ann	Pre-irrad	Post-irrad	Post-ann
5318	300 krad	4	13	4	24	254	102
5319	300 krad	5	15	5	24	252	81
5320	300 krad	7	17	8	25	222	69
5321	200 krad	5	6	5	24	71	32
5355	200 krad	5	6	5	25	76	34
5356	200 krad	4	6	5	24	83	34

Based on these PIPL, post-annealed DUT passes both the ICCA and ICCI spec for 200 krad (SiO₂).

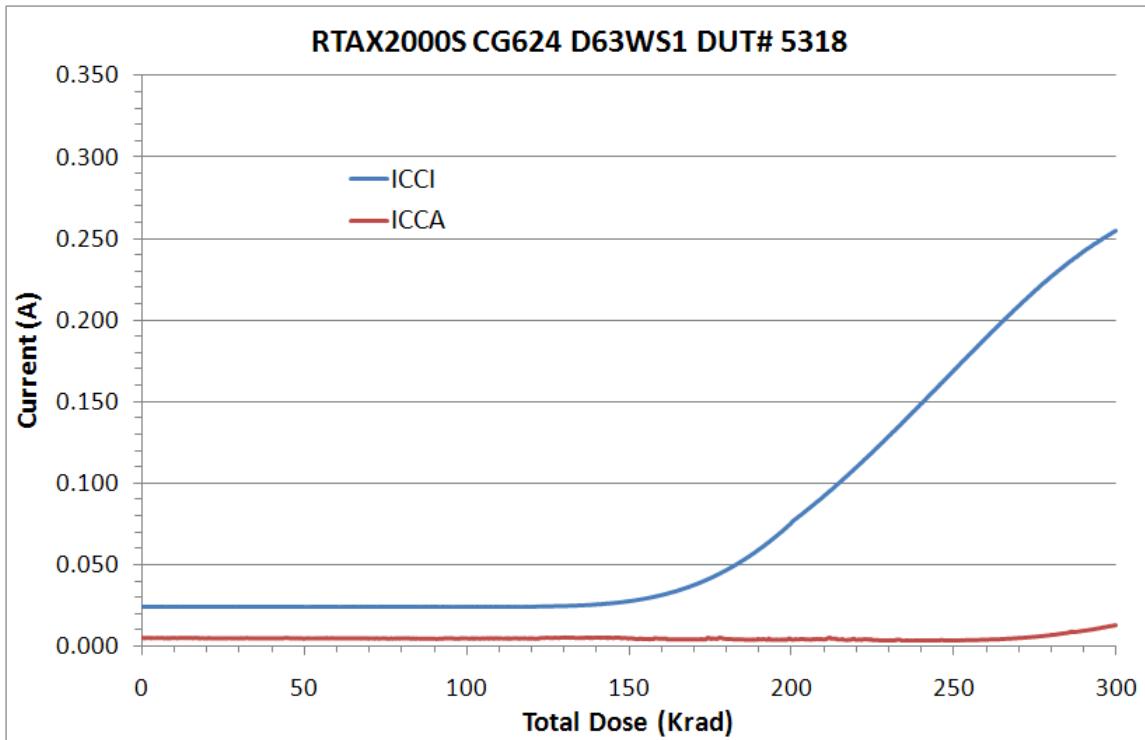


Figure 2 DUT 5318 Influx ICCA and ICCI

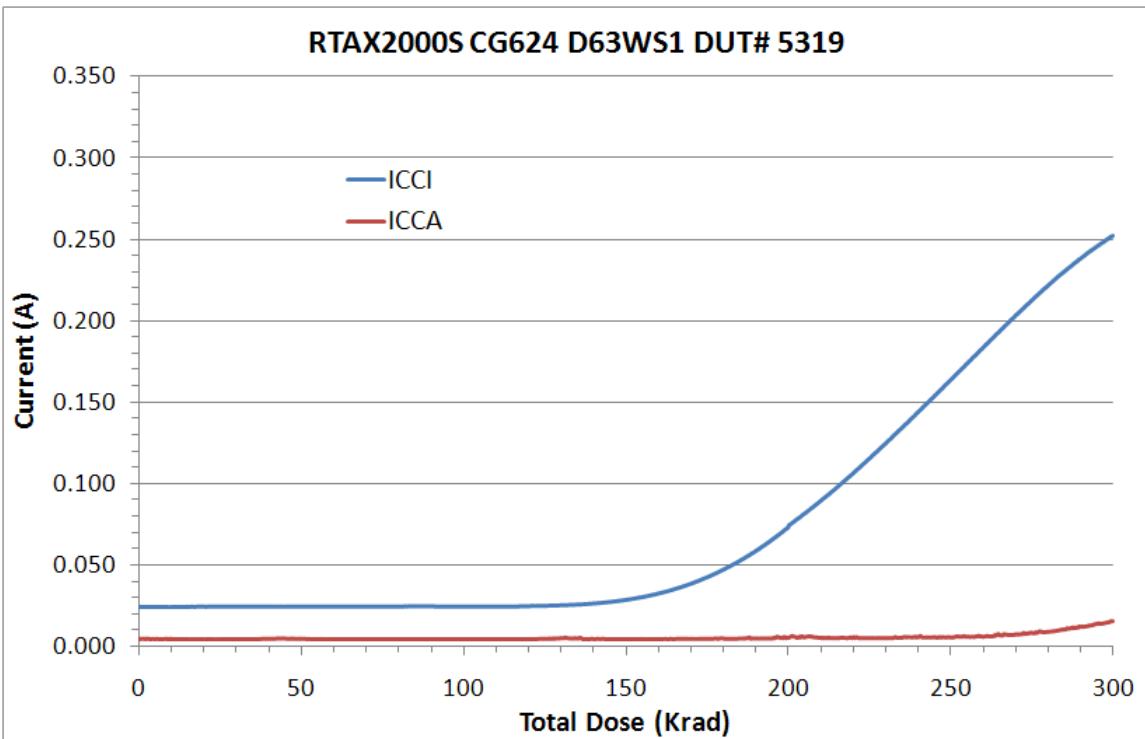


Figure 3 DUT 5319 Influx ICCA and ICCI

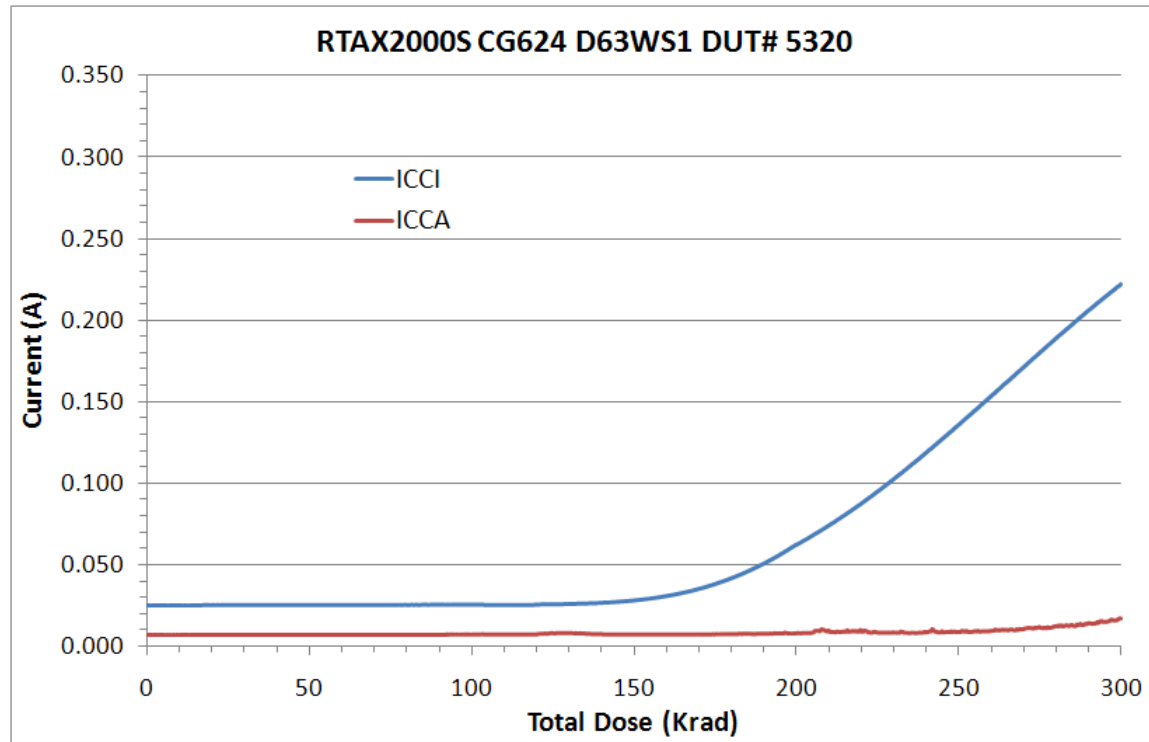


Figure 4 DUT 5320 Influx ICCA and ICCI

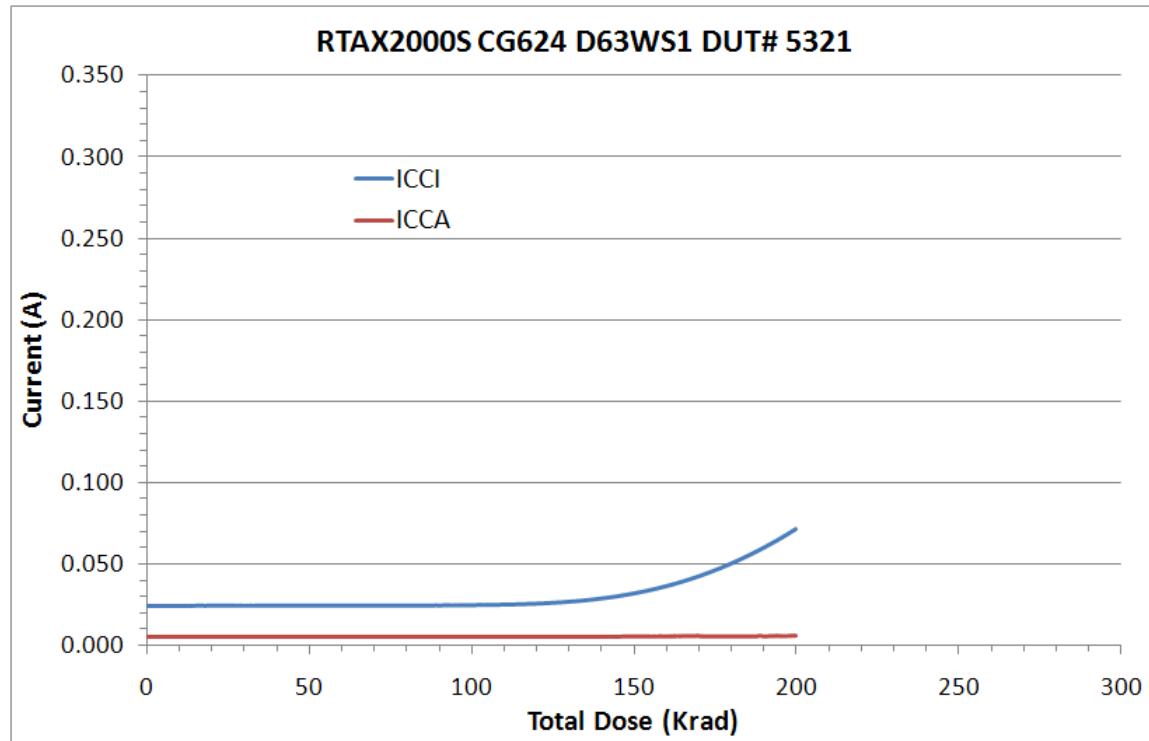


Figure 5 DUT 5321 Influx ICCA and ICCI

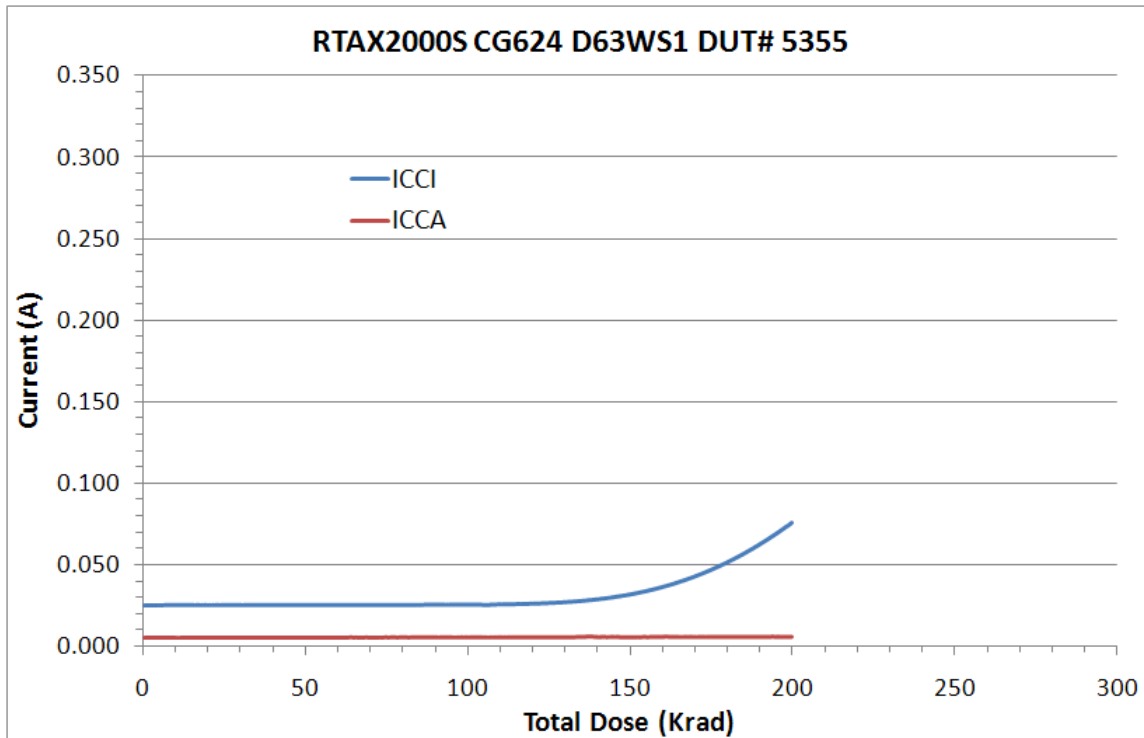


Figure 6 DUT 5355 Influx ICCA and ICCI

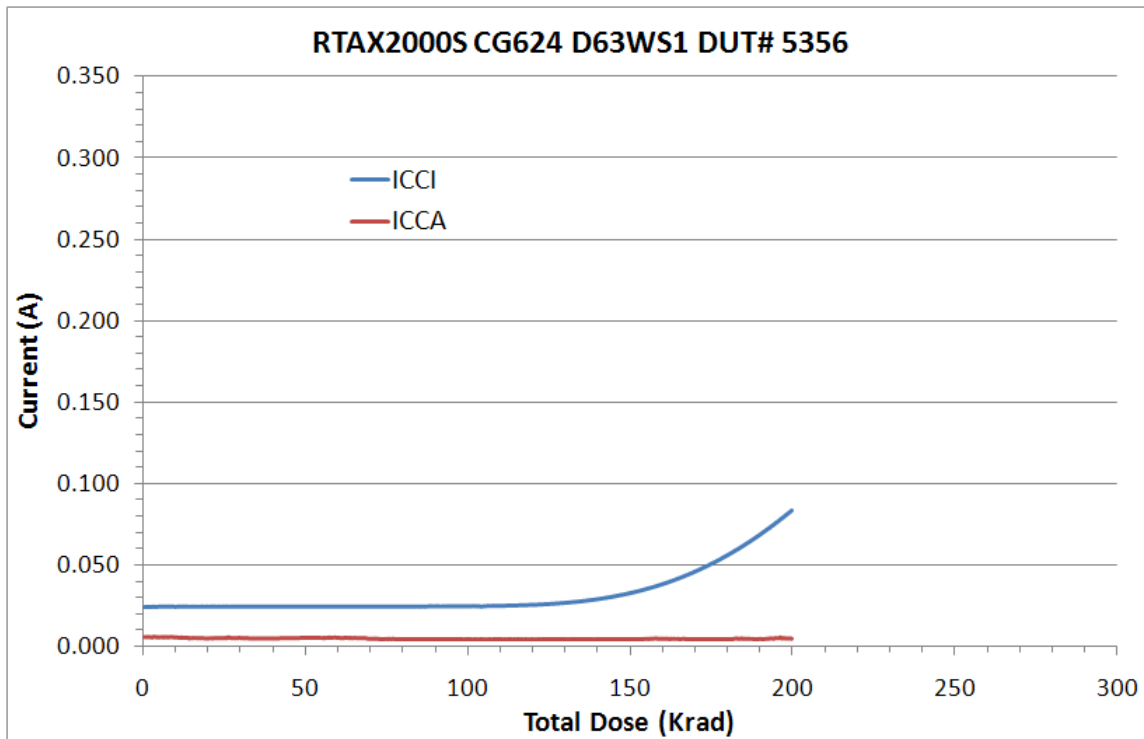


Figure 7 DUT 5356 Influx ICCA and ICCI

C. Single-Ended Input Logic Threshold (VIL/VIH)

Table 3a through Table 3c list the pre-irradiation and post-annealing single-ended input logic thresholds. All data are within the specification limits. The post-annealing shift in every case is very small.

Table 3a Pre-Irradiation and Post-Annealing Input Thresholds

DUT	5318 (300 krad)				5319 (300 krad)				
	Input Pin	Pre-Irrad	Post-Ann	Pre-Irrad	Post-Ann	Pre-Irrad	Post-Ann	Pre-Irrad	Post-Ann
		VIL (mV)		VIH (mV)		VIL (mV)		VIH (mV)	
Bi_D_7	Bi_D_7	1390	1380	1390	1380	1390	1380	1390	1385
Bi_D_6	Bi_D_6	1375	1365	1400	1390	1365	1360	1390	1390
Bi_D_5	Bi_D_5	1380	1370	1395	1385	1385	1375	1395	1385
Bi_D_4	Bi_D_4	1390	1380	1390	1380	1385	1375	1385	1380
Bi_D_3	Bi_D_3	1385	1375	1400	1390	1380	1375	1395	1395
Bi_D_2	Bi_D_2	1375	1365	1400	1390	1370	1370	1390	1385
Bi_D_1	Bi_D_1	1375	1365	1395	1385	1380	1365	1395	1385
DA	DA	1385	1385	1415	1405	1380	1385	1415	1400
EN8	EN8	1355	1355	1420	1410	1355	1340	1425	1405
IO_I_6	IO_I_6	1365	1355	1440	1425	1355	1355	1430	1425
IO_I_5	IO_I_5	1370	1360	1445	1420	1360	1345	1420	1435
IO_I_4	IO_I_4	1420	1405	1410	1400	1410	1405	1400	1395
IO_I_3	IO_I_3	1400	1395	1415	1405	1385	1385	1410	1405
IO_I_2	IO_I_2	1410	1400	1405	1395	1410	1405	1405	1400
IO_I_1	IO_I_1	1405	1395	1415	1405	1400	1395	1410	1405
RCLK1P	RCLK1P	1445	1440	1440	1430	1445	1440	1440	1435
RCLK2P	RCLK2P	1440	1440	1440	1435	1445	1440	1445	1440

Table 3b Pre-Irradiation and Post-Annealing Input Thresholds

DUT	5320 (300 krad)				5321 (200 krad)				
	Input Pin	Pre-Irrad	Post-Ann	Pre-Irrad	Post-Ann	Pre-Irrad	Post-Ann	Pre-Irrad	Post-Ann
		VIL (mV)		VIH (mV)		VIL (mV)		VIH (mV)	
Bi_D_7	1385	1375	1385	1375	1375	1365	1375	1370	
Bi_D_6	1365	1355	1390	1385	1360	1355	1385	1380	
Bi_D_5	1380	1365	1390	1380	1375	1365	1385	1380	
Bi_D_4	1380	1370	1380	1370	1375	1370	1380	1370	
Bi_D_3	1375	1365	1395	1385	1375	1365	1390	1380	
Bi_D_2	1370	1360	1390	1385	1365	1360	1390	1380	
Bi_D_1	1370	1360	1390	1380	1365	1355	1380	1375	
DA	1395	1365	1410	1400	1385	1360	1395	1395	
EN8	1345	1330	1460	1450	1340	1335	1450	1415	
IO_I_6	1365	1355	1430	1365	1355	1350	1425	1420	
IO_I_5	1360	1340	1425	1430	1360	1340	1440	1425	
IO_I_4	1410	1390	1400	1390	1400	1395	1395	1390	
IO_I_3	1385	1385	1410	1395	1395	1375	1400	1395	
IO_I_2	1410	1395	1405	1390	1400	1390	1395	1385	
IO_I_1	1400	1395	1410	1400	1390	1385	1400	1395	
RCLK1P	1440	1435	1435	1425	1440	1435	1435	1430	
RCLK2P	1440	1435	1435	1430	1440	1440	1435	1435	

Table 3c Pre-Irradiation and Post-Annealing Input Thresholds

DUT	5355 (200 krad)				5356 (200 krad)				
	Input Pin	Pre-Irrad	Post-Ann	Pre-Irrad	Post-Ann	Pre-Irrad	Post-Ann	Pre-Irrad	Post-Ann
		VIL (mV)		VIH (mV)		VIL (mV)		VIH (mV)	
Bi_D_7	1370	1365	1370	1365	1375	1370	1375	1370	
Bi_D_6	1355	1350	1380	1370	1365	1355	1385	1380	
Bi_D_5	1370	1360	1380	1375	1370	1365	1385	1375	
Bi_D_4	1375	1365	1375	1365	1375	1365	1375	1365	
Bi_D_3	1365	1355	1380	1375	1375	1365	1390	1380	
Bi_D_2	1360	1350	1380	1375	1365	1355	1385	1375	
Bi_D_1	1360	1350	1380	1370	1360	1355	1380	1370	
DA	1385	1355	1400	1395	1385	1360	1400	1395	
EN8	1335	1330	1450	1445	1340	1330	1405	1420	
IO_I_6	1355	1345	1420	1415	1355	1345	1425	1415	
IO_I_5	1355	1335	1430	1395	1350	1350	1420	1430	
IO_I_4	1390	1385	1385	1380	1400	1395	1395	1390	
IO_I_3	1395	1385	1400	1395	1380	1385	1400	1395	
IO_I_2	1395	1390	1390	1385	1395	1395	1395	1390	
IO_I_1	1390	1385	1400	1395	1390	1395	1400	1395	
RCLK1P	1440	1435	1435	1430	1440	1440	1435	1430	
RCLK2P	1440	1440	1440	1435	1440	1440	1440	1440	

D. Differential Input (LVPECL) Threshold Voltage (VIL/VIH)

Table 4a through Table 4c list the LVPECL differential input threshold voltage changes due to irradiations. All pins show negligible changes, and all the data are within the specification.

Table 4a Pre-Irradiation and Post-Annealing Differential Input Thresholds

DUT	5318 (300 krad)				5319 (300 krad)			
	Input Pin		Pre-Irrad	Post-Ann	Pre-Irrad	Post-Ann	Pre-Irrad	Post-Ann
			VIL (mV)		VIH (mV)		VIL (mV)	
DIO_IP_7	100	80	95	80	105	100	100	100
DIO_IP_6	115	95	110	95	105	105	105	105
DIO_IP_5	110	90	105	90	110	95	110	95
DIO_IP_4	85	65	80	65	95	75	95	75
DIO_IP_3	85	70	85	70	90	85	90	85
DIO_IP_2	85	70	80	65	80	85	80	80
DIO_IP_1	80	65	90	70	80	65	85	65

Table 4b Pre-Irradiation and Post-Annealing Differential Input Thresholds

DUT	5320 (300 krad)				5321 (200 krad)			
	Input Pin		Pre-Irrad	Post-Ann	Pre-Irrad	Post-Ann	Pre-Irrad	Post-Ann
			VIL (mV)		VIH (mV)		VIL (mV)	
DIO_IP_7	105	85	100	85	90	85	90	80
DIO_IP_6	105	95	105	90	100	95	95	90
DIO_IP_5	110	95	110	95	100	95	95	90
DIO_IP_4	90	75	90	75	95	85	90	85
DIO_IP_3	95	80	95	80	80	75	80	75
DIO_IP_2	90	75	85	75	90	85	90	85
DIO_IP_1	80	65	90	65	80	75	85	80

Table 4c Pre-Irradiation and Post-Annealing Differential Input Thresholds

DUT	5355 (200 krad)				5356 (200 krad)			
	Input Pin		Pre-Irrad	Post-Ann	Pre-Irrad	Post-Ann	Pre-Irrad	Post-Ann
			VIL (mV)		VIH (mV)		VIL (mV)	
DIO_IP_7	110	105	110	105	100	95	100	95
DIO_IP_6	100	90	95	90	115	105	110	105
DIO_IP_5	110	105	110	105	105	95	100	95
DIO_IP_4	75	70	75	70	85	80	85	75
DIO_IP_3	80	75	80	70	85	80	85	80
DIO_IP_2	90	85	90	85	90	85	85	80
DIO_IP_1	80	70	85	75	75	70	85	70

E. Output-Drive Voltage (VOL/VOH)

The pre-irradiation and post-annealing VOL/VOH are listed in Table 5a through Table 5c. The post-annealing data are within the specification limits.

Table 5a Pre-Irradiation and Post-Annealing VOL and VOH

DUT	5318 (300 krad)				5319 (300 krad)				
	Input Pin	Pre-Irrad	Post-Ann	Pre-Irrad	Post-Ann	Pre-Irrad	Post-Ann	Pre-Irrad	Post-Ann
VOL (mV)		VOH (mV)		VOL (mV)		VOH (mV)			
Bi_IO_7	35	35	2965	2965	35	35	2970	2965	
Bi_IO_6	30	30	2965	2960	30	30	2965	2965	
Bi_IO_5	35	35	2965	2965	35	35	2965	2965	
Bi_IO_4	30	35	2965	2965	30	35	2965	2965	
Bi_IO_3	30	35	2965	2965	30	35	2970	2965	
Bi_IO_2	35	35	2970	2965	35	35	2970	2965	
Bi_IO_1	35	35	2965	2965	35	35	2965	2965	
Bi_Y_7	25	25	2980	2980	25	25	2985	2980	
Bi_Y_6	25	25	2980	2980	25	25	2980	2980	
Bi_Y_5	30	30	2980	2980	30	30	2980	2980	
Bi_Y_4	25	25	2980	2980	25	25	2980	2980	
Bi_Y_3	25	25	2980	2980	25	25	2980	2980	
Bi_Y_2	20	25	2980	2980	20	25	2980	2980	
Bi_Y_1	25	30	2980	2980	25	30	2980	2980	
CLOCK	20	20	2970	2970	20	20	2970	2970	
CLOCK	20	25	2970	2970	20	20	2970	2970	
QA_2	20	20	2970	2965	20	20	2970	2970	
QA_1	20	20	2970	2965	0	20	2970	2965	
QA_0	0	20	2970	2970	0	20	2970	2970	

Table 5b Pre-Irradiation and Post-Annealing VOL and VOH

DUT	5320 (300 krad)				5321 (200 krad)				
	Input Pin	Pre-Irrad	Post-Ann	Pre-Irrad	Post-Ann	Pre-Irrad	Post-Ann	Pre-Irrad	Post-Ann
		VOL (mV)		VOH (mV)		VOL (mV)		VOH (mV)	
Bi_IO_7	35	35	2965	2965	35	35	2965	2970	
Bi_IO_6	30	30	2965	2965	30	30	2965	2965	
Bi_IO_5	35	35	2965	2965	35	35	2965	2970	
Bi_IO_4	30	35	2965	2965	30	35	2965	2965	
Bi_IO_3	30	35	2965	2965	30	35	2965	2965	
Bi_IO_2	35	30	2970	2965	30	30	2970	2965	
Bi_IO_1	35	35	2965	2965	35	35	2965	2965	
Bi_Y_7	25	25	2980	2980	25	25	2980	2980	
Bi_Y_6	25	25	2980	2980	25	25	2980	2985	
Bi_Y_5	25	25	2980	2980	25	25	2980	2985	
Bi_Y_4	25	25	2980	2980	25	25	2980	2980	
Bi_Y_3	25	25	2980	2980	25	25	2980	2980	
Bi_Y_2	25	25	2980	2980	25	25	2980	2980	
Bi_Y_1	25	30	2980	2980	25	30	2980	2980	
CLOCK	20	20	2970	2970	20	20	2970	2970	
CLOCK	20	20	2970	2970	20	25	2970	2970	
QA_2	0	20	2970	2965	20	20	2970	2965	
QA_1	20	20	2970	2970	20	20	2970	2970	
QA_0	20	20	2970	2970	20	20	2970	2970	

Table 5c Pre-Irradiation and Post-Annealing VOL and VOH

DUT Input Pin	5355 (200 krad)				5356 (200 krad)			
	Pre-Irrad	Post-Ann	Pre-Irrad	Post-Ann	Pre-Irrad	Post-Ann	Pre-Irrad	Post-Ann
	VOL (mV)		VOH (mV)		VOL (mV)		VOH (mV)	
Bi_IO_7	35	35	2970	2970	35	35	2965	2970
Bi_IO_6	30	30	2965	2965	30	30	2965	2965
Bi_IO_5	35	35	2970	2965	35	35	2970	2970
Bi_IO_4	30	35	2965	2965	35	35	2965	2965
Bi_IO_3	30	30	2965	2965	35	35	2965	2960
Bi_IO_2	35	30	2970	2965	30	30	2970	2965
Bi_IO_1	35	35	2965	2965	35	35	2965	2965
Bi_Y_7	25	25	2980	2980	25	25	2980	2980
Bi_Y_6	25	25	2980	2980	25	25	2980	2985
Bi_Y_5	25	25	2980	2985	30	25	2980	2985
Bi_Y_4	25	25	2980	2980	25	25	2980	2980
Bi_Y_3	25	25	2980	2980	25	25	2980	2980
Bi_Y_2	20	25	2980	2980	20	25	2980	2980
Bi_Y_1	25	30	2980	2980	25	30	2980	2980
CLOCK	20	20	2970	2970	20	20	2970	2970
CLOCK	20	25	2970	2970	20	25	2970	2970
QA_2	0	20	2970	2970	20	20	2970	2965
QA_1	0	20	2970	2970	0	20	2970	2970
QA_0	20	20	2970	2970	20	20	2970	2970

F. Propagation Delay

The propagation delay was measured in-situ, post-irradiation, and post-annealing. The irradiation was temporarily stopped at each total-dose increment of 100 krad for the measurement. The results are plotted in Figure 8, and listed in Table 6. As shown in Figure 8, the propagation delay initially decreases with the total dose, but the change is small throughout the irradiation. Referring to influx static current plots (Figure 2 through Figure 7), a device probably heats up as the dose increases. The rising temperature could be the root cause of the increasing trend at high doses. The post-annealing data, on the other hand, show decreased delay in every case.

The radiation delta in every case is well within the 10% degradation criterion. User can take the worst case for the design-margin consideration.

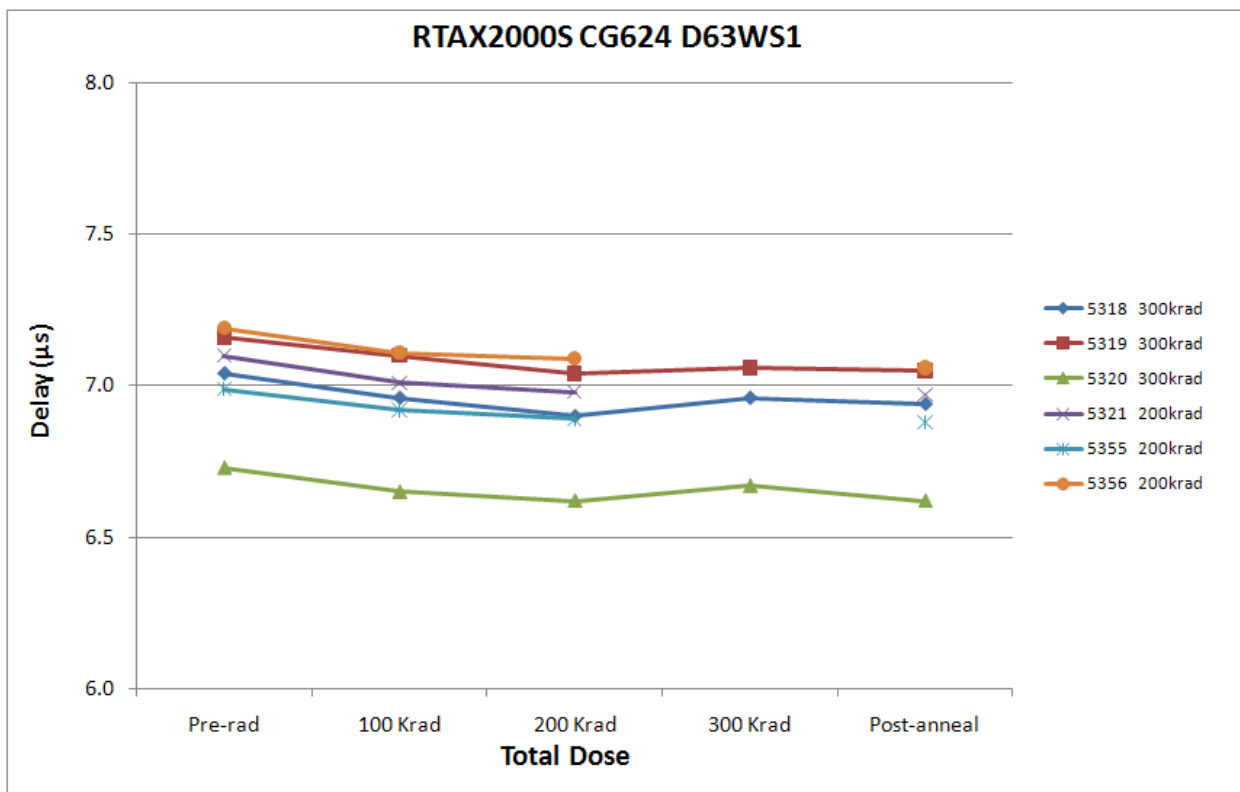


Figure 8 In-Situ Propagation Delay versus Total Dose

Table 6 Radiation-Induced Propagation-Delay Degradations

	RTAX2000S CG624 D63WS1						
Delay (μs)							
	DUT	Total Dose	Pre-rad	100 krad	200 krad	300 krad	Post-ann
5318	300 krad	7.04	6.96	6.90	6.96	6.94	
	300 krad	7.16	7.10	7.04	7.06	7.05	
	300 krad	6.73	6.65	6.62	6.67	6.62	
	200 krad	7.10	7.01	6.98	-	6.97	
	200 krad	6.99	6.92	6.89	-	6.88	
	200 krad	7.19	7.11	7.09	-	7.06	
Radiation Δ (%)							
	DUT	Total Dose	Pre-rad	100 krad	200 krad	300 krad	Post-ann
5318	300 krad	-	-1.14%	-1.99%	-1.14%	-1.42%	
	300 krad	-	-0.84%	-1.68%	-1.40%	-1.54%	
	300 krad	-	-1.19%	-1.63%	-0.89%	-1.63%	
	200 krad	-	-1.27%	-1.69%	-	-1.83%	
	200 krad	-	-1.00%	-1.43%	-	-1.57%	
	200 krad	-	-1.11%	-1.39%	-	-1.81%	

G. Transition Characteristics

Figure 9a to Figure 20b show the pre-irradiation and post-annealing transition edges. In each case, the radiation-induced transition-time degradation is insignificant.

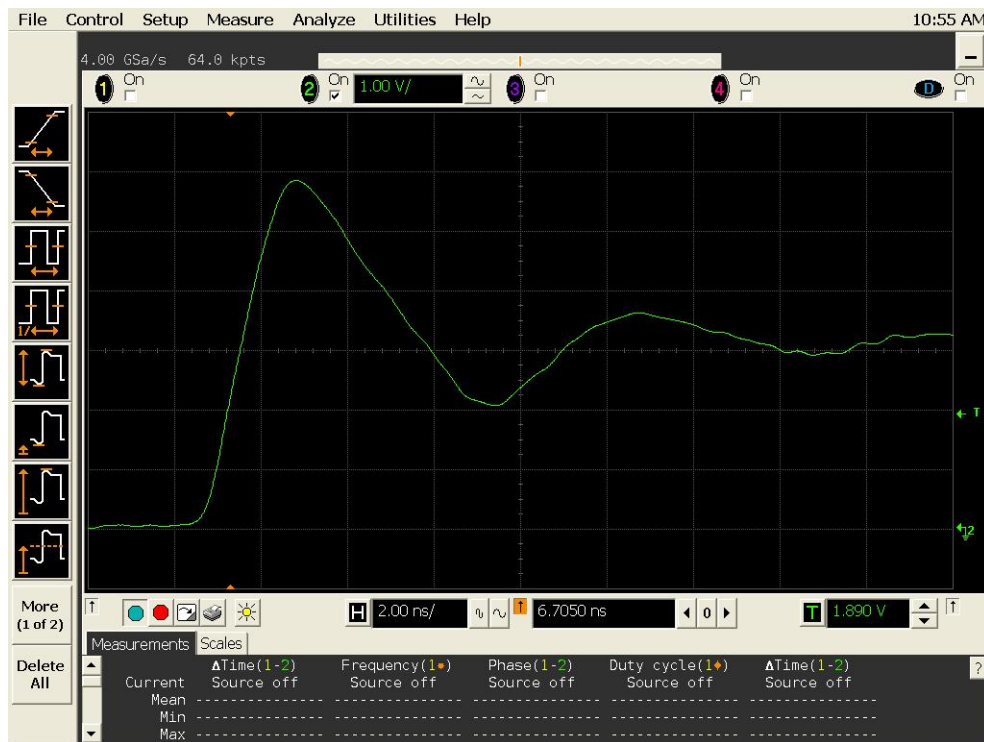


Figure 9a DUT 5318 Pre-Irradiation Rising Edge

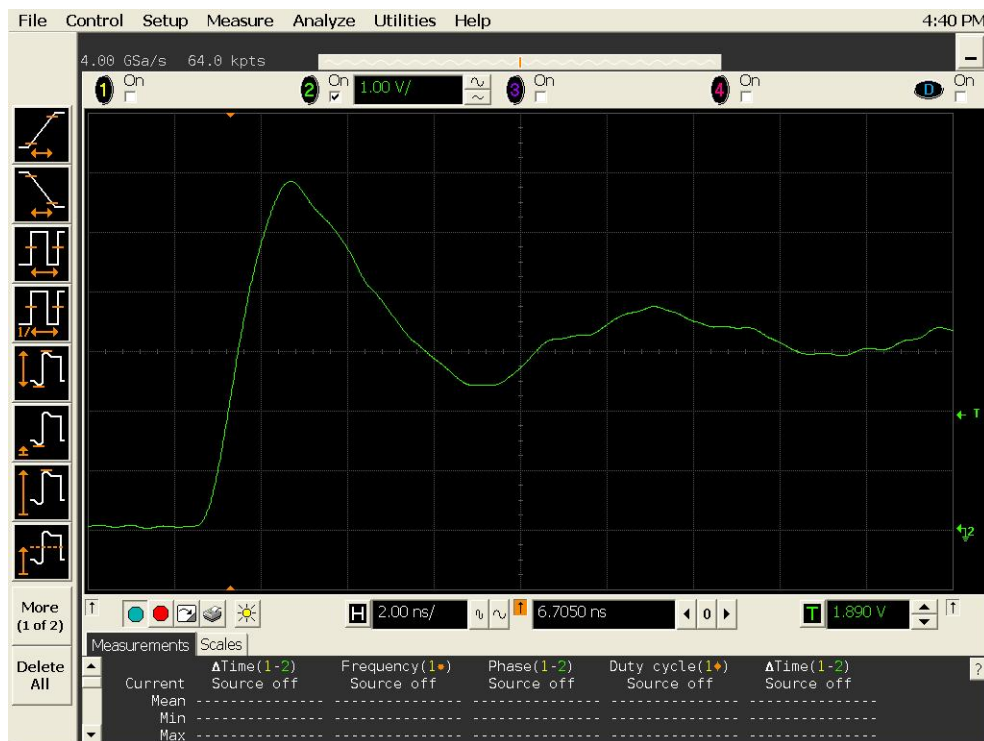


Figure 9b DUT 5318 Post-Annealing Rising Edge

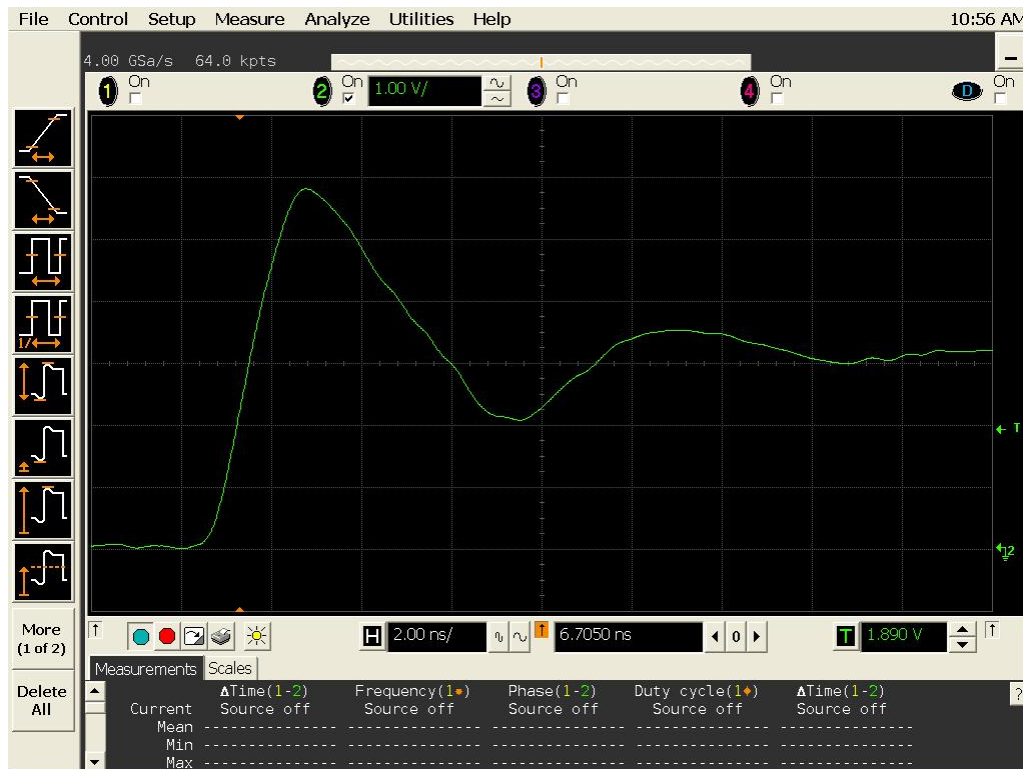


Figure 10a DUT 5319 Pre-Irradiation Rising Edge



Figure 10b DUT 5319 Post-Annealing Rising Edge

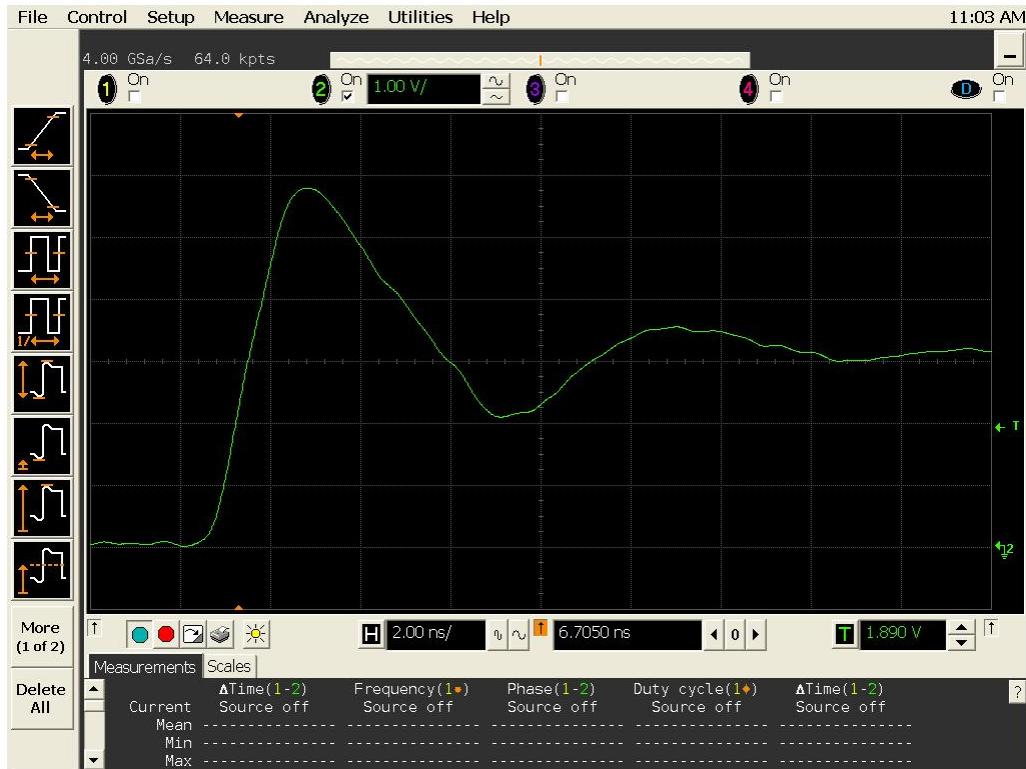


Figure 11a DUT 5320 Pre-Radiation Rising Edge

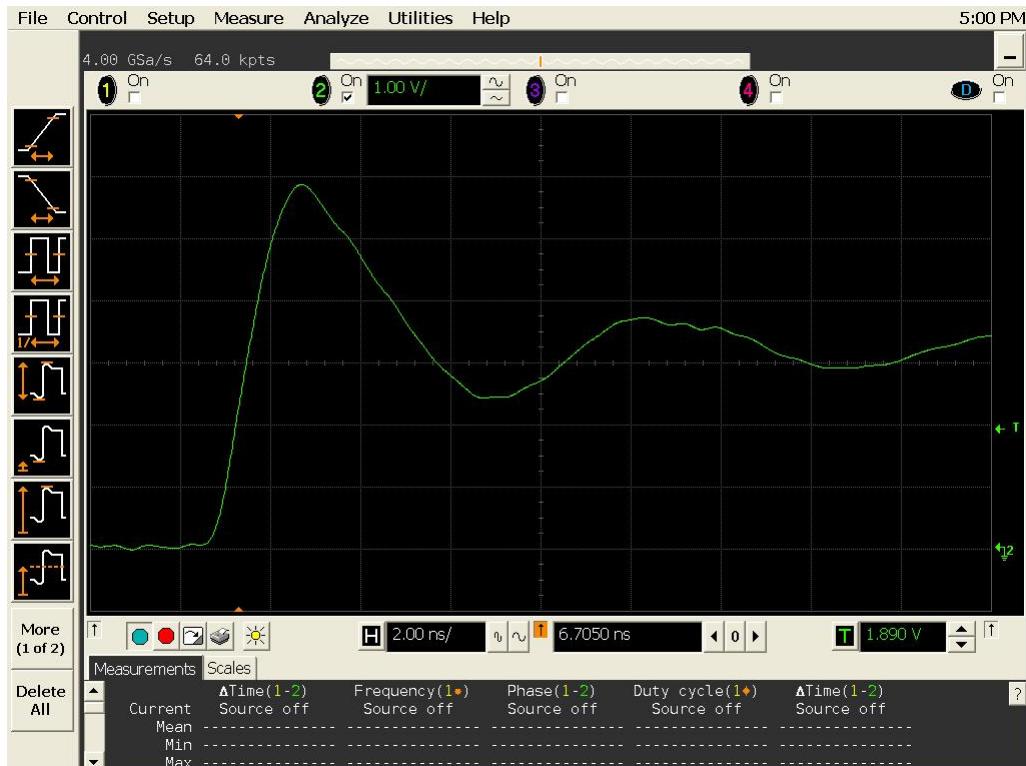


Figure 11b DUT 5320 Post-Annealing Rising edge

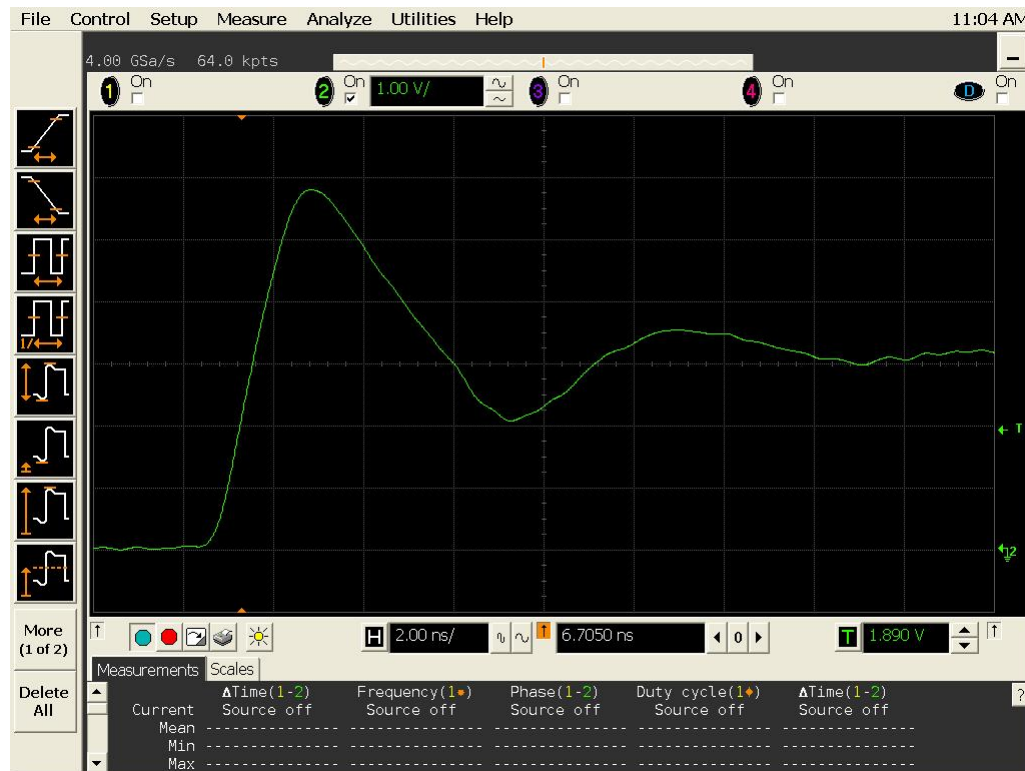


Figure 12a DUT 5321 Pre-Irradiation Rising Edge

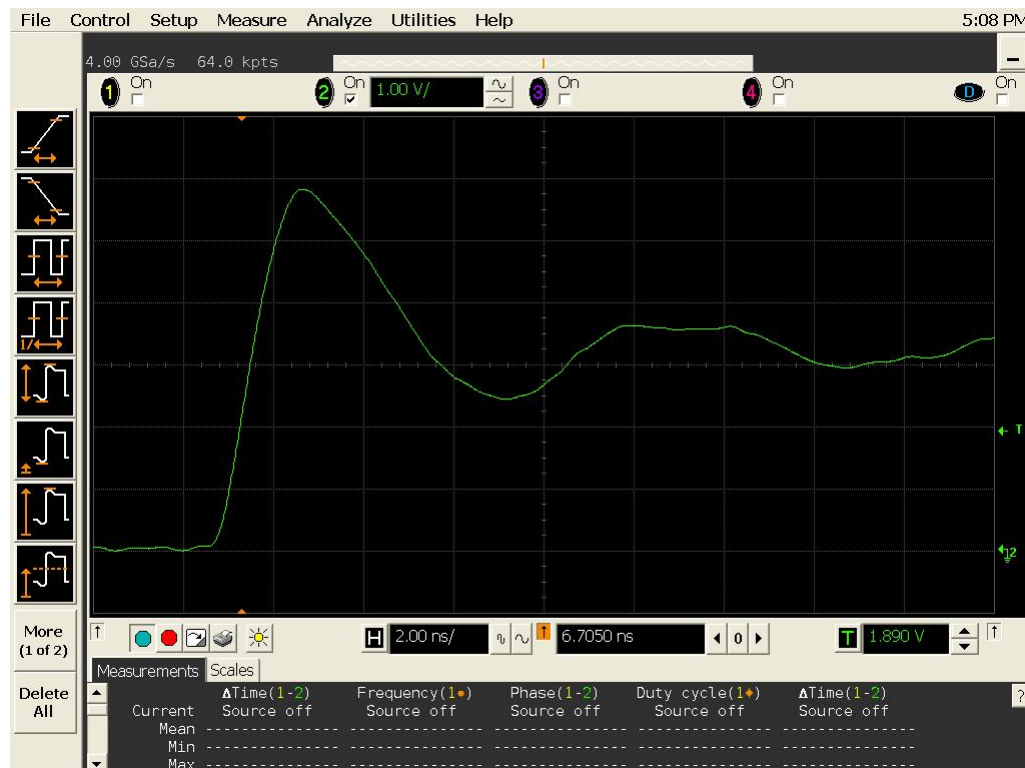


Figure 12b DUT 5321 Post-Annealing Rising Edge

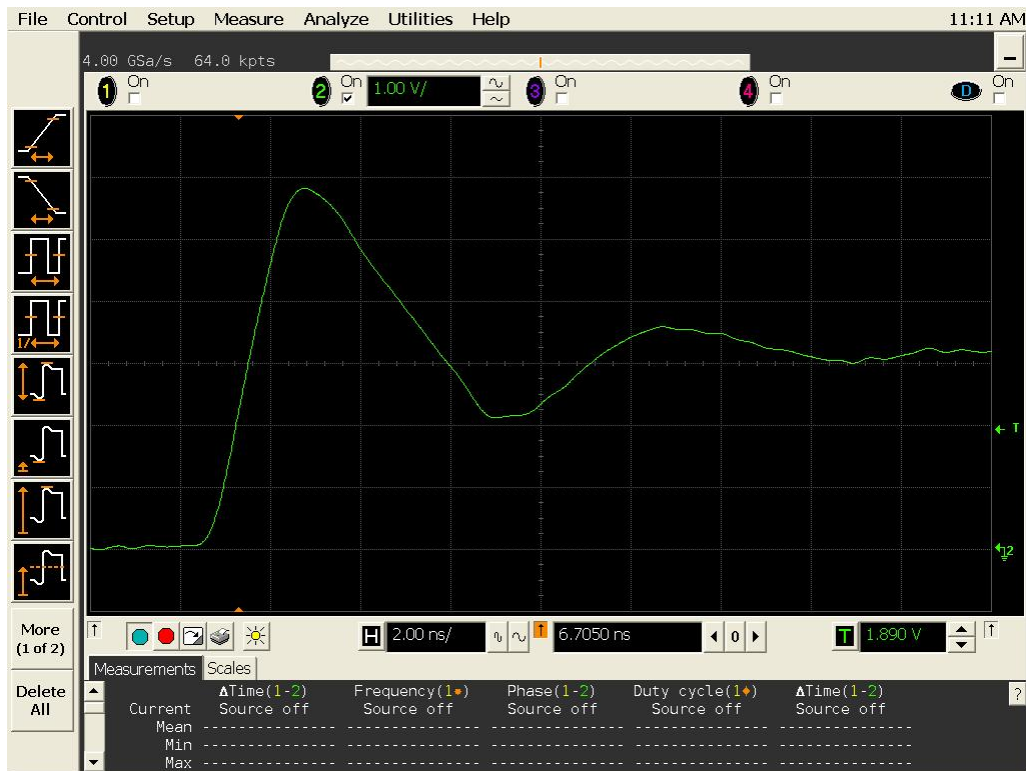


Figure 13a DUT 5355 Pre-Irradiation Rising Edge

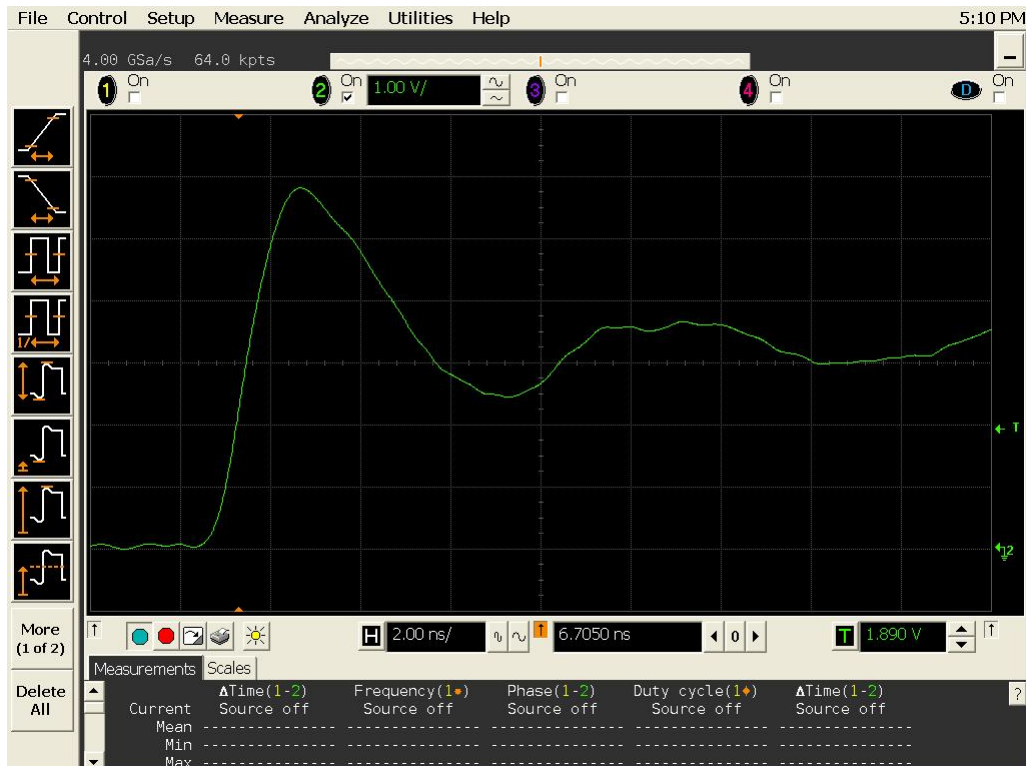


Figure 13b DUT 5355 Post-Annealing Rising Edge

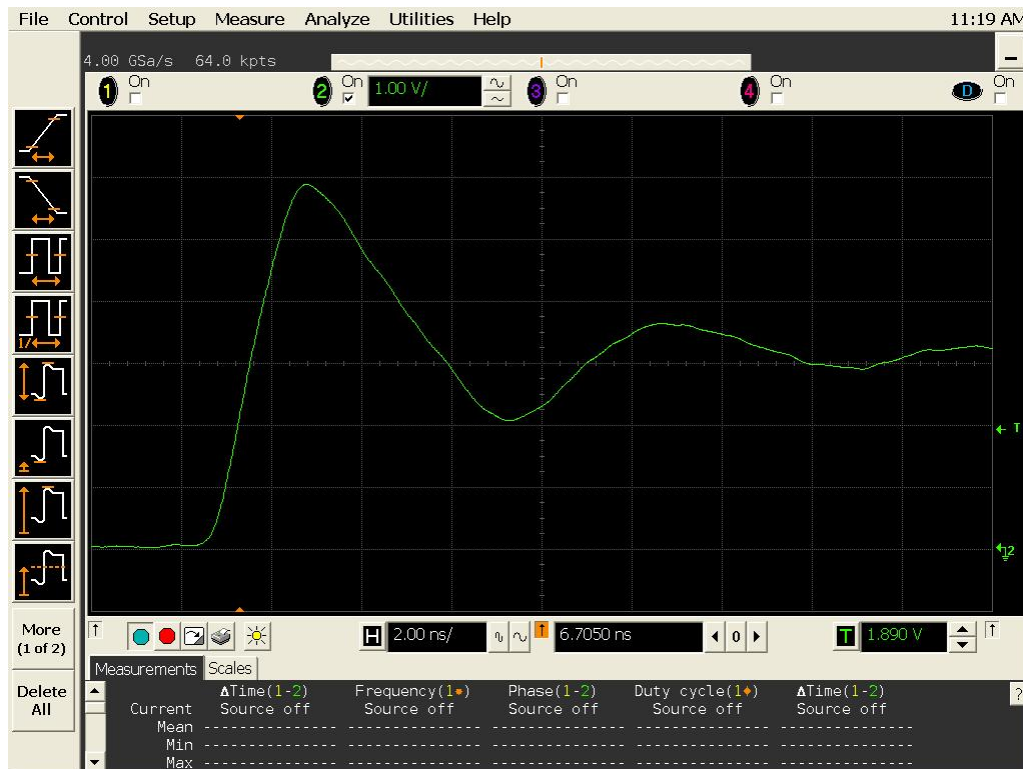


Figure 14a DUT 5356 Pre-Irradiation Rising Edge

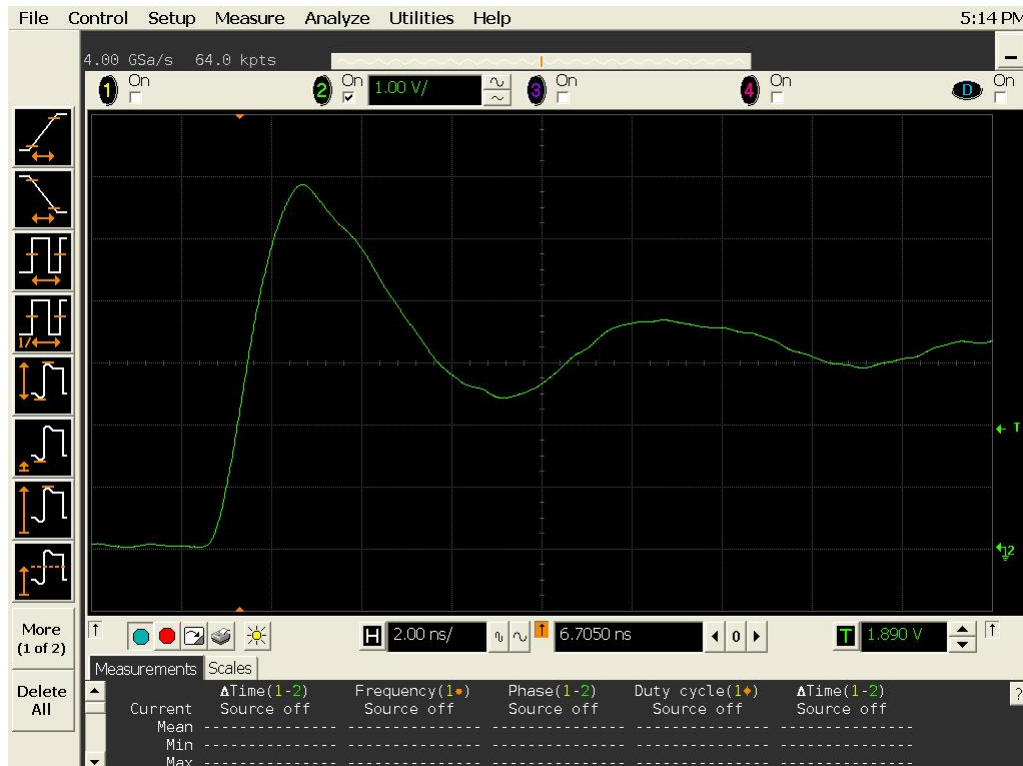


Figure 14b DUT 5356 Post-Annealing Rising Edge



Figure 15a DUT 5318 Pre-Radiation Falling Edge

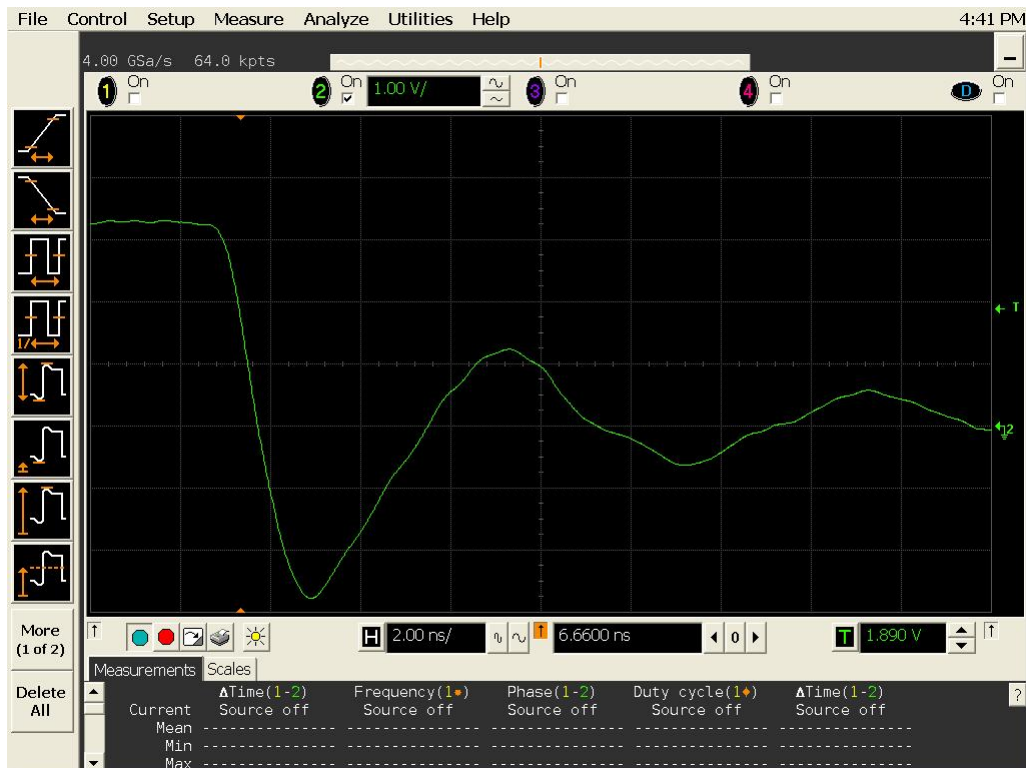


Figure 15b DUT 5318 Post-Annealing Falling Edge



Figure 16a DUT 5319 Pre-Irradiation Falling Edge



Figure 16b DUT 5319 Post-Annealing Falling Edge

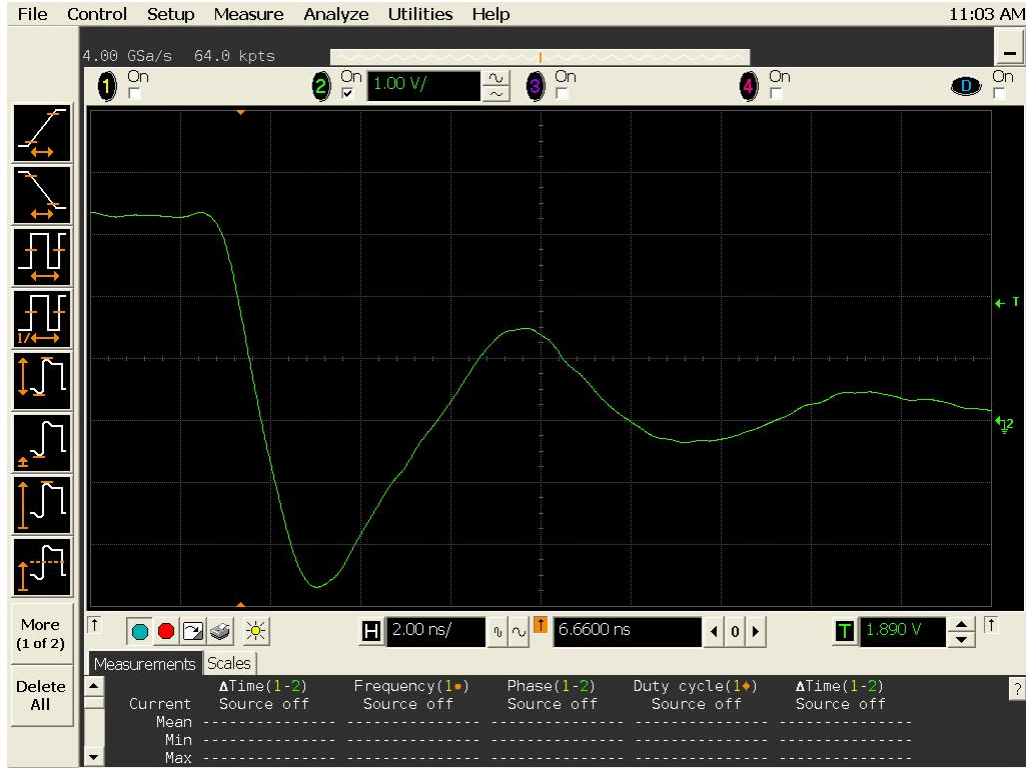


Figure 17a DUT 5320 Pre-Irradiation Falling Edge

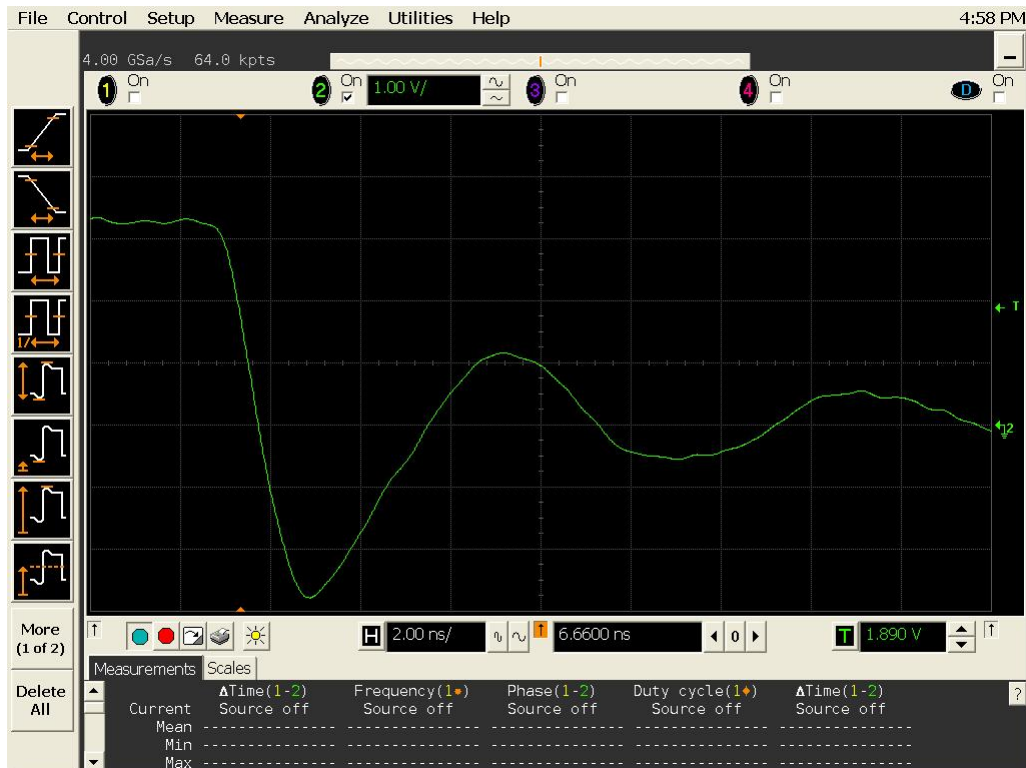


Figure 17b DUT 5320 Post-Annealing Falling Edge



Figure 18a DUT 5321 Pre-Irradiation Falling Edge

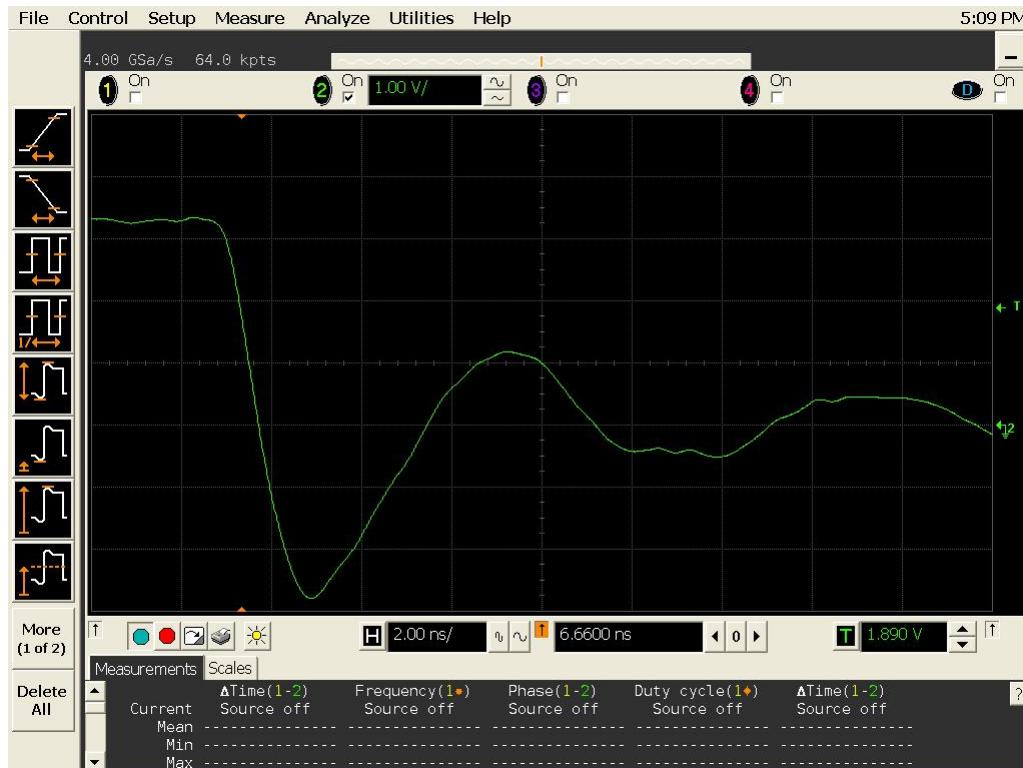


Figure 18b DUT 5321 Post-Annealing Falling Edge



Figure 19a DUT 5355 Pre-Irradiation Falling Edge



Figure 19b DUT 5355 Post-Annealing Falling Edge



Figure 20a DUT 5356 Pre-Irradiation Falling Edge

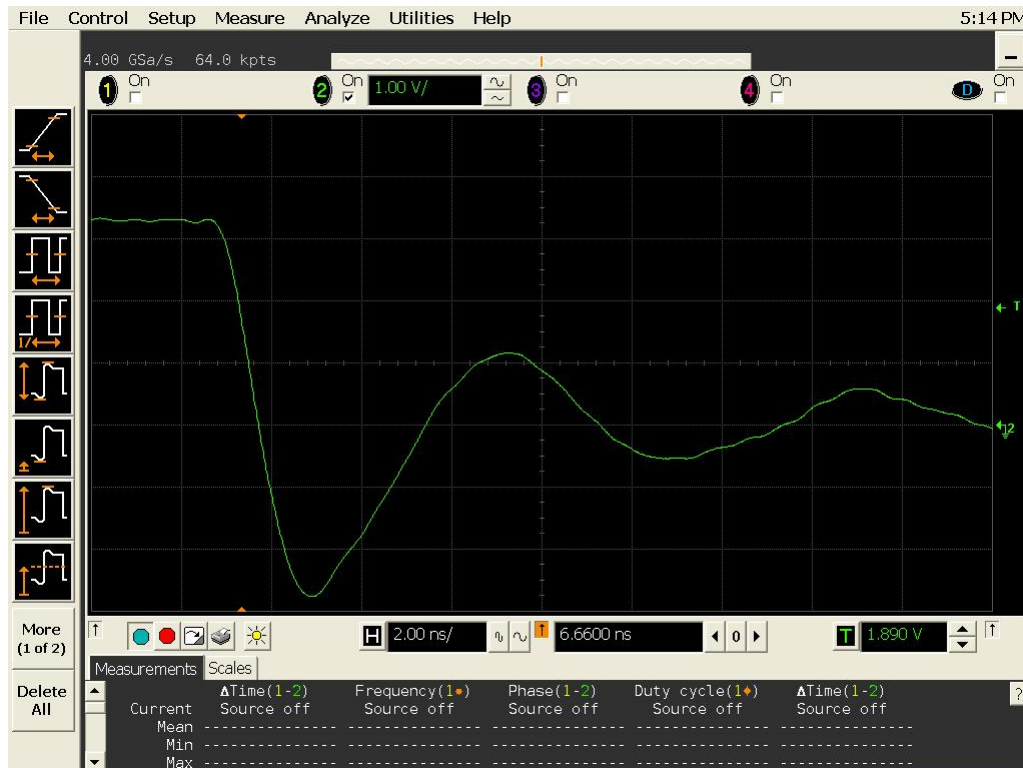
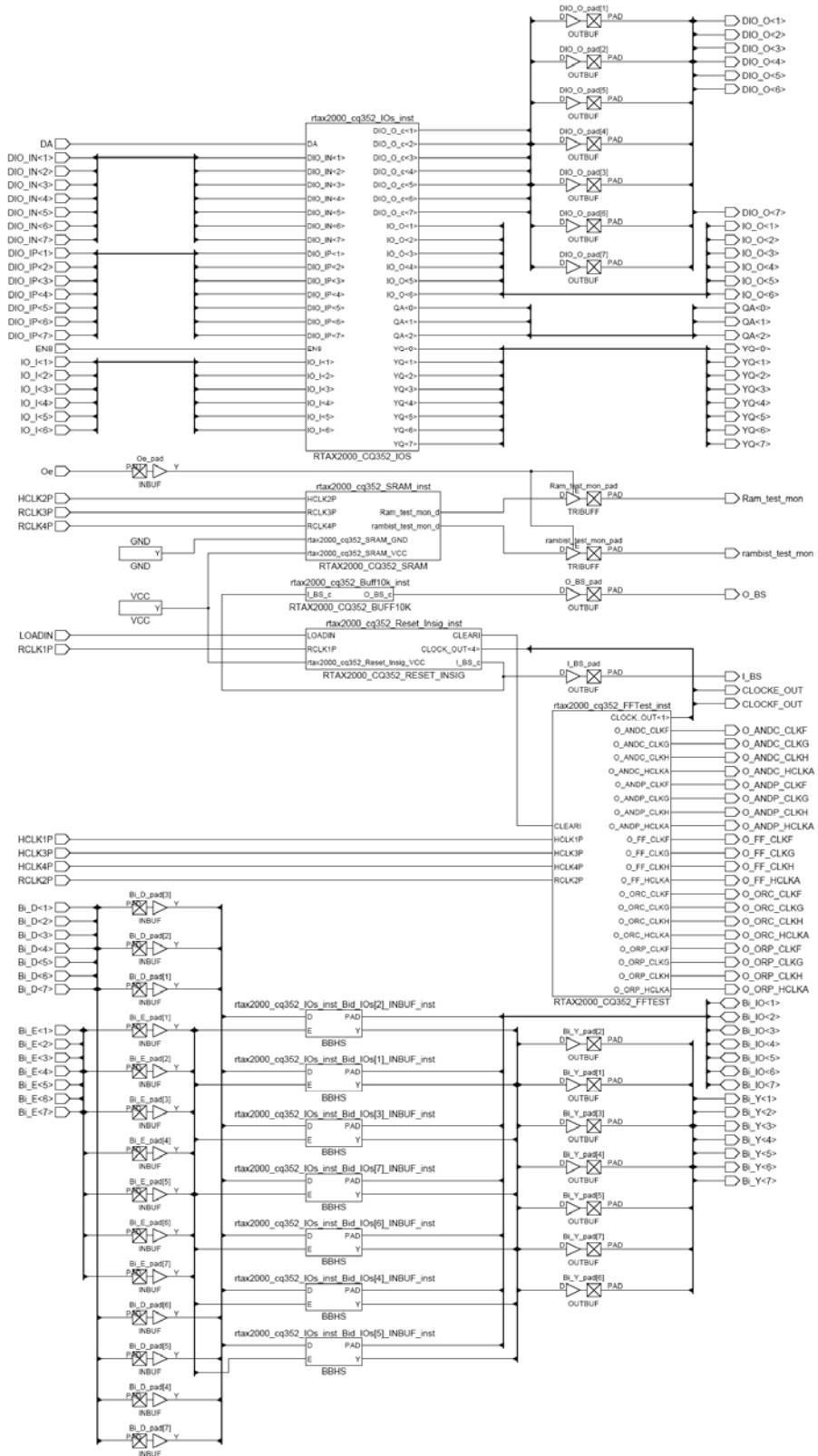


Figure 20b DUT 5356 Post-Annealing Falling Edge

Appendix A: DUT Design Schematics





Microsemi Corporate Headquarters
One Enterprise, Aliso Viejo CA 92656 USA
Within the USA: +1 (949) 380-6100
Sales: +1 (949) 380-6136
Fax: +1 (949) 215-4996

Microsemi Corporation (NASDAQ: MSCC) offers a comprehensive portfolio of semiconductor solutions for: aerospace, defense and security; enterprise and communications; and industrial and alternative energy markets. Products include high-performance, high-reliability analog and RF devices, mixed signal and RF integrated circuits, customizable SoCs, FPGAs, and complete subsystems. Microsemi is headquartered in Aliso Viejo, Calif. Learn more at www.microsemi.com.

© 2012 Microsemi Corporation. All rights reserved. Microsemi and the Microsemi logo are trademarks of Microsemi Corporation. All other trademarks and service marks are the property of their respective owners.